



**HAL**  
open science

## Red phosphorus/aluminium oxide compositions as flame retardants in recycled poly(ethylene terephthalate)

Fouad Laoutid, Laurent Ferry, José-Marie Lopez-Cuesta, Alain Crespy

### ► To cite this version:

Fouad Laoutid, Laurent Ferry, José-Marie Lopez-Cuesta, Alain Crespy. Red phosphorus/aluminium oxide compositions as flame retardants in recycled poly(ethylene terephthalate). *Polymer Degradation and Stability*, 2003, 82 (2), pp.357-363. 10.1016/S0141-3910(03)00213-1 . hal-03269471

**HAL Id: hal-03269471**

**<https://imt-mines-ales.hal.science/hal-03269471>**

Submitted on 11 Nov 2021

**HAL** is a multi-disciplinary open access archive for the deposit and dissemination of scientific research documents, whether they are published or not. The documents may come from teaching and research institutions in France or abroad, or from public or private research centers.

L'archive ouverte pluridisciplinaire **HAL**, est destinée au dépôt et à la diffusion de documents scientifiques de niveau recherche, publiés ou non, émanant des établissements d'enseignement et de recherche français ou étrangers, des laboratoires publics ou privés.



Distributed under a Creative Commons Attribution 4.0 International License

# Red phosphorus/aluminium oxide compositions as flame retardants in recycled poly(ethylene terephthalate)

F. Laoutid, L. Ferry, J.M. Lopez-Cuesta\*, A. Crespy

*Centre des Matériaux de Grande Diffusion (C.M.G.D), Ecole des Mines d'Alès, 6, Avenue de Clavières 30319 Alès Cedex, France*

## Abstract

The mechanical properties and fire resistance of a recycled poly(ethylene terephthalate) were improved by using a specific treatment of the waste material and the incorporation of encapsulated red phosphorus in combination with co-additives. The use of red phosphorus has to be limited due to a negative influence on impact resistance and rate of heat release. Among several metal oxides,  $\text{Al}_2\text{O}_3$  acts as a good co-synergist at a total loading of 5 wt.% due to its reactivity, high specific surface area and aluminium phosphate formation. The complementary use of glass fibres can also generate intumescence by improving the mechanical stability of the char layer.

*Keywords:* PET recycling; Fire resistance; Red phosphorus; Aluminium oxide; Intumescence

## 1. Introduction

The main applications of reclaimed poly(ethylene terephthalate) (PET) bottles after regeneration are fibres, packaging, strips and films [1]. The re-use of PET in technical applications is limited. This can be explained by the difficulty of reprocessing PET and the need to confer new properties in order to obtain engineered plastics.

Some indications were given by Muller et al. [2] concerning the decrease in molecular weight for recycled PET in comparison with virgin PET. This phenomenon is ascribed to chain breakages due to the presence of traces of water and acidic impurities.

The objectives of this work were to prepare a PET with controlled mechanical properties (by drying and elimination of impurities) from a commercial recycled PET, and to improve its resistance to flammability.

Encapsulated red phosphorus was chosen as a flame retardant because of:

- its flame retardant (FR) action in oxygen-containing polymers;

- its effectiveness at low percentages in polymers;
- the possibility of working safe from phosphine emission thanks to encapsulation; and
- the existence of synergists.

Our study will also focus on the mechanisms of thermal degradation and flammability of recycled PET containing flame retardants and co-synergists.

## 2. Experimental

### 2.1. Materials

The PET flakes were supplied by the Valorplast Company, which is in charge of the collection of post-use waste packaging in France.

Red phosphorus encapsulated in PA 6 was provided by Italmatch. The composition of the masterbatch is 50% w/w of each component.

Two types of aluminium oxide were used:

1. Nabalox NO 713-10, median particle size = 0.5  $\mu\text{m}$ , specific surface area = 7–14  $\text{m}^2/\text{g}$ .
2. Calcined alumina trihydrate Martinal OL 104 (Martinswerk); the non-calcined raw material has a median particle size of 2.5  $\mu\text{m}$  and a specific surface area of 4  $\text{m}^2/\text{g}$ .

\* Corresponding author. Tel.: +33-4-6678-5241; fax: +33-4-6678-5201.

*E-mail address:* jose-marie.lopez-cuesta@ema.fr (J.M. Lopez-Cuesta).

Magnesium oxide was obtained by calcination of magnesium hydroxide Magnifin H10 (Martinswerk). The median particle size of the raw material is 1  $\mu\text{m}$  with a BET surface area of 9.5–11  $\text{m}^2/\text{g}$ .

Iron oxide was supplied by Panreac with a median particle size of 2.5  $\mu\text{m}$  and a specific surface area of 8  $\text{m}^2/\text{g}$ . Glass fibres were incorporated using a commercial PET–glass fibre composite (Rynite 530 from Du Pont); their median length and diameter are respectively, 300 and 10  $\mu\text{m}$ . Talc, Mistron RP6, was supplied by Luzenac Europe (median particle size = 2.5  $\mu\text{m}$  and specific surface area = 11  $\text{m}^2/\text{g}$ ).

## 2.2. Techniques

### 2.2.1. Compositions, blending and processing

Red phosphorus was incorporated into recycled PET up to a value of 5 wt.%. Metal oxides were incorporated in partial substitution of red phosphorus; the total loading was kept constant at 5%. Glass fibres and talc were incorporated at 6% w/w percentage in addition to the FR system (red phosphorus alone or with metal oxides).

Red phosphorus and reinforced glass fibre masterbatches were diluted in PET flakes prior to their incorporation in an injection-moulding device (Sandretto Otto 95 T). Masterbatches of metal oxides with PET were made by twin-screw extrusion (Clextral BC 21) and blended with red phosphorus masterbatches prior to injection moulding. The processing temperatures were 260–280  $^{\circ}\text{C}$  depending on the compositions.

The specimens produced were dogbones according to ISO 527-2 type 1A specifications and used for mechanical testing, 100 $\times$ 100 $\times$ 4 mm sheets were used for flammability tests.

Metal oxides were blended with PET flakes in a twin-screw extruder Clextral BC 21 to make a 30% w/w masterbatch before dilution with PET and injection moulding.

### 2.3. Physical and chemical characterization

#### 2.3.1. Thermal degradation and flammability

Thermal analysis and specific flammability experiments were carried out to characterize the thermal behaviour of PET. Thermal degradation studies were performed using a differential thermogravimetric and thermal analyser (Setaram TGDTA92). The temperature profile used was 5  $^{\circ}\text{C}/\text{min}$  from 25 to 700  $^{\circ}\text{C}$ . The PET crystallinity was determined using a differential scanning calorimeter Setaram DSC92.

Flammability tests [Limiting Oxygen Index: LOI (ISO 4589) and the epiradiateur test (AFNOR NF P 92-505)] were also used. The LOI test indicates the minimal percentage of oxygen in an oxygen/nitrogen flow which corresponds to a stable combustion of a specimen. In

the epiradiateur test, a 70 $\times$ 70 $\times$ 4 mm sheet is placed on a metallic grid below a 500 W radiator; the radiator is removed and replaced (respectively) after each ignition and extinguishing. The first time of ignition and the mean and maximal values of combustion times are determined. At least four specimens were tested for each composition.

The thermal behaviour was also tested by a cone calorimeter device (Fire Testing Technology). A 100 $\times$ 100 $\times$ 4 mm sheet is exposed to a radiant cone (150  $\text{kw}/\text{m}^2$ ). The rate of heat release (RHR) can be calculated as a function of the oxygen consumption linked to the combustion of the specimen using an oxygen analyser.

### 2.4. Thermomechanical and mechanical characterization

Rheological measurements were carried out at 260  $^{\circ}\text{C}$  on PET compositions using an Ares Rheometrics apparatus. Viscosity was measured in the dynamic regime in the shear rate range from 10 $^{-1}$  to 10 $^2$   $\text{rad s}^{-1}$ . Maximum tensile strength of dogbones was measured according to the ISO 178 standard using an Adamel Lhomargy universal testing machine. Unnotched Charpy impact strength was determined using a Zwick apparatus according to ISO 179 standard.

### 2.5. Spectroscopic and microscopic characterization

Broken cross-sections of specimens and combustion char residues were observed and studied using a SEM Jeol 35CF and an EDX device. Crystalline mineral structures were identified by means of a Philips X-ray diffractometer. The chemical structure of the residue was also studied by FTIR spectroscopy (Brüker IFS 66). FTIR was also coupled with a TG analyser in order to analyse the gases emitted during thermal decomposition. The integration of specific features of the IR spectrum as a function of time provides a specific curve called the Gram Schmidt curve [3,4].

## 3. Results and discussion

### 3.1. Incorporation of red phosphorus in a PET with mechanically controlled properties

The chemical analysis of the recycled PET revealed that it contains remaining impurities such as paper and non-miscible plastics (mainly PVC). This leads to a material showing poor elongation at break and impact resistance values (Table 1). The material also exhibits low viscosity due to a well-known hydrolysis phenomenon [5] occurring during the processing of non-dried PET.

Consequently, in order to obtain a PET with controlled properties, the following process was carried out:

Table 1  
Mechanical properties and limiting oxygen values of filled and unfilled recycled PET

Sample	Elongation at break (%)	Maximal tensile strength (MPa)	Impact resistance (kJ/m <sup>2</sup> )	LOI (%)
PET 0	2.61±0.7	49.8±10.6	24.1±9.5	23.5
PET 1	> 150	58.5±3.2	> 187	23.5
PET 2	> 150	59±2.4	> 187	23.5
PET + 5% Red P	> 150	54.8±0.8	92.6±4.8	35.5
PET + 3% Red P	> 150	55±1.3	> 187	29.9

- impurities (paper and PVC) were eliminated by manual sorting after calcination for 8 h in an oven at 160 °C; and
- the purified PET was then carefully dried in a vacuum oven at 160 °C for 16 h.

The tensile properties and impact resistance of the resulting PET (PET1) were compared, on the one hand, to those of the initial PET (PET0) and on the other hand, to those of PET flakes (PET2). This last material was obtained by grinding bottles collected locally in which the plastic part covered by the label was eliminated. It can be noticed in Table 1 that the values of elongation at break and impact resistance for PET 1 and 2 are significantly higher than those obtained for PET 0. All the incorporations of flame retardants (FR) were then made using PET 1.

The incorporation of increasing amounts of red phosphorus (red P) up to 5% w/w seems to have a positive effect on the tensile properties of recycled PET. One can notice that only a slight decrease in maximum tensile strength is observed, while values of elongation at break are in a similar range and can even be improved at low percentages of red P (Table 1). The incorporation of red P also tends continuously to increase PET viscosity when the FR percentage is increased. Nevertheless, impact resistance is damaged, particularly from to 3% (Table 1). The observation of

broken cross-sections by SEM (Fig. 1) reveals that red P acts as a filler in PET. Red P/PET adhesion seems poor; moreover the large size of red P particles (median diameter higher than 10 microns) may also explain the decrease of impact resistance with increasing percentages of red P.

The analysis of TG curves of recycled PET both in air and argon indicates that in both cases the decomposition is a two-step process (Fig. 2). The first step is very rapid (occurring in the 370–430 °C range) and corresponds to the main decomposition. The second step corresponds to the decomposition of the char residue. In an argon atmosphere, this residue is stable up to 700 °C whereas in air the mass loss is complete at this temperature.

The incorporation of red P at percentages of 3 and 5% in recycled PET was studied using TGA in airflow. Fig. 2 shows that red P accelerates the decomposition of PET by increasing the first step kinetics, but red P also tends to promote the formation of a residue (char) stable up to 650 °C. Gram Schmidt curves for combustible gases (Fig. 3) also show this acceleration in the emission of volatiles, but they also show that these emissions are strongly reduced with the formation of the char. Its formation in air atmosphere can be linked to the mechanisms of the action of red P in polymers.

These mechanisms have been described by several authors [6,7] who emphasized that the processes occurring in the condensed phase are predominant, the presence of oxygen leading to the formation of a

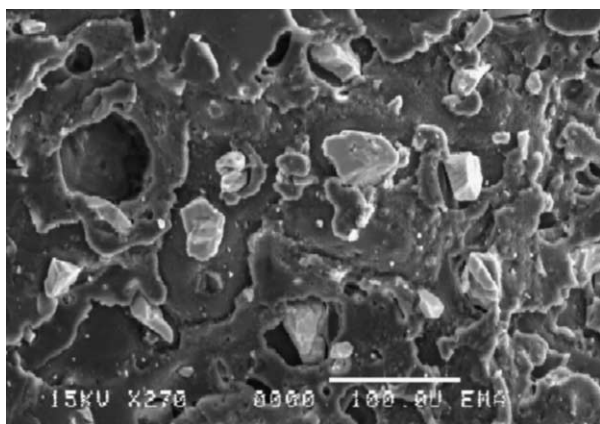


Fig. 1. SEM micrograph (×270) of broken cross sections of filled PET (5% red P).

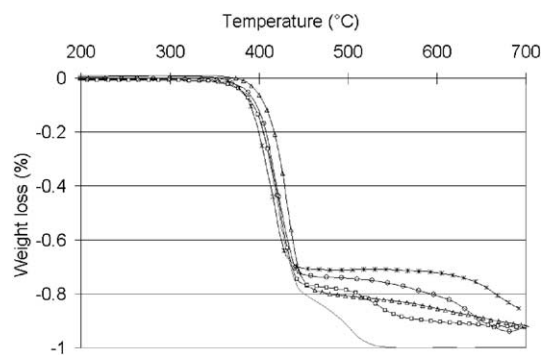


Fig. 2. TGA curves of filled and unfilled PET in air and argon (5 °C/min). (—) PET in air, (Δ) PET in Argon, (□) 3% red P, (\*) 5% red P, (○) 3% red P + 2% Al<sub>2</sub>O<sub>3</sub>.

phosphorus anhydride with increasing temperature. Phosphoric acid is then formed followed by the formation of phosphoric polyacid causing dehydration of PET and char formation. The mechanism in the gaseous phase corresponds to the formation of phosphorus monoxide ( $P=O$ ), which is able to react with free radicals ( $H^\circ$  and  $OH^\circ$ ) and thus to decrease the combustion rate. Fig. 2 confirms the predominance of this condensed phase mechanism since the TG curves of PET containing 5% red P are quite similar in both air and argon. Moreover, red P could also improve the mechanical stability of the char layer formed during combustion. This phenomenon was connected with the increase of the shear viscosity of PET with increasing percentages of red P (Fig. 4). This increase of viscosity could limit the flowing of molten polymer during the first stages of degradation and favour the stability of the char.

The incorporation of red P tends also to improve the resistance to flammability since it increases the LOI values which increase continuously from 23 to 35% for unfilled PET and PET containing 5% red P, respectively (Table 1). Nevertheless, the increase of LOI at 5% is not enough to predict good overall fire behaviour for PET incorporating red P. The RHR values measured using a cone calorimeter (Fig. 5) correspond to a decrease of RHR peak of PET, however, the RHR peak is higher

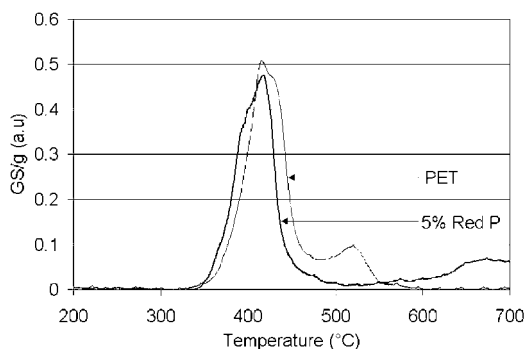


Fig. 3. Gram Schmidt curves of unfilled PET and PET with 5% red phosphorus as a function of temperature.

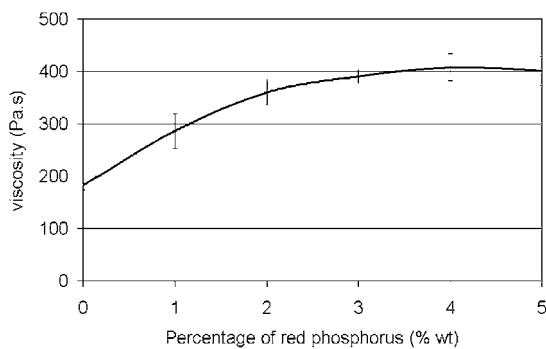


Fig. 4. Shear viscosity of PET as a function of the percentage of red phosphorus.

for 5% red P than in the case of 3% red P. This evolution seems to confirm the phenomenon observed by Weil [8] who mentioned that in some polymers a maximum LOI at a certain % red P is observed; however, this author did not give a reason. The acceleration of PET decomposition due to the introduction of red P and the creation of the char could act as an antagonism in relation to material flammability. The limitation in use of red P due to this increase in RHR peak and the observed decrease in impact strength may suggest the use of co-synergists able to limit the drawbacks caused by the incorporation of relatively high amounts of red P in recycled PET.

### 3.2. Incorporation of metal oxides in combination with red P

The objectives of the incorporation of metallic oxides are based on the search for synergists for improving flammability properties. These products may be involved in several mechanisms:

- action on PET viscosity in the molten state, which could mechanically stabilize the char;
- catalytic action on degradation products promoting char formation; and
- oxidation of red phosphorus or phosphorus compounds.

Moreover the relatively high cost of red P encourages the use of relatively low cost substitution compounds also acting as synergists.

A previous study on the combination of red P with some metallic oxides ( $MgO$  and  $Al_2O_3$ ) was made by Yeh et al. [9]. Nevertheless, the mechanisms of action of these oxides was not fully explained and the role of their morphology was not studied.

We substituted different metal oxides for some of the red P. Among these oxides,  $MgO$ ,  $Al_2O_3$  (obtained from calcination of trihydrated alumina) and  $Fe_2O_3$  exhibited

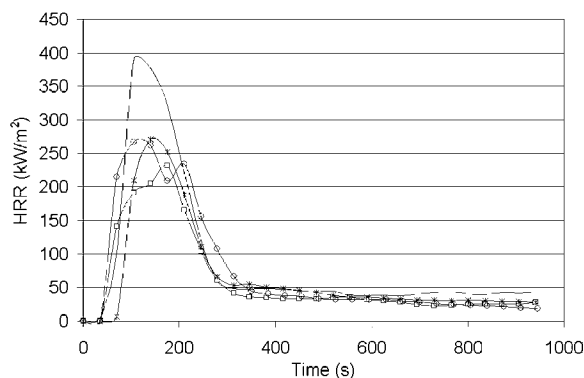


Fig. 5. Heat Release Rate of filled and unfilled PET as a function of time. (—) PET, (□) 3% red P, (\*) 5% red P, (○) 3% red P+2%  $Al_2O_3$ .

a synergistic action referring to LOI measurements. Fig. 6 shows that the synergism is the most active for 2% red P/3% oxide compositions in the case of  $\text{Fe}_2\text{O}_3$  and for 3% red P/2% oxide compositions in the case of  $\text{Al}_2\text{O}_3$  and  $\text{MgO}$ . A TG thermogram in air (Fig. 2) shows a comparison for the compositions containing 3 and 5% red P and that in which 2% red P was replaced by  $\text{Al}_2\text{O}_3$ . It can be observed that the presence of  $\text{Al}_2\text{O}_3$  does not slow down the increase in the decomposition rate due to red P. The incorporation of  $\text{Al}_2\text{O}_3$  also tends to stabilize the char by increasing the weight of residue at 600 °C.

The synergistic action of  $\text{Al}_2\text{O}_3$  can also be noticed in RHR curves. The RHR peak and RHR values over a large range of time decreases significantly when  $\text{Al}_2\text{O}_3$  is substituted for 2% red P (Fig. 5).

Increased viscosity was one hypothesis put forward to explain the action of these oxides on PET flammability. Nevertheless, no significant variation in rheology compared with unfilled PET was noticed. The second hypothesis concerned a catalytic action of oxides. Nevertheless, it may be also possible that the oxides

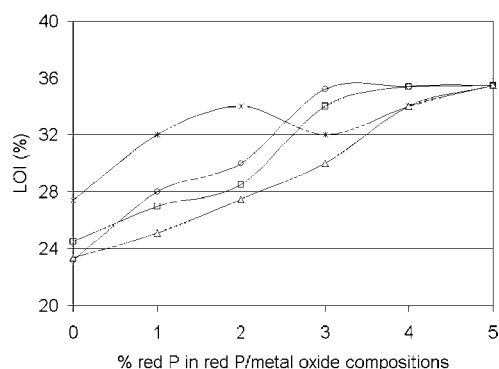


Fig. 6. Limiting oxygen index (LOI) of PET as a function of the red P/metal oxide composition. (□) red P/ $\text{Al}_2\text{O}_3$ , (○) red P/ $\text{MgO}$ , (\*) red P/ $\text{Fe}_2\text{O}_3$ , (△) red P.

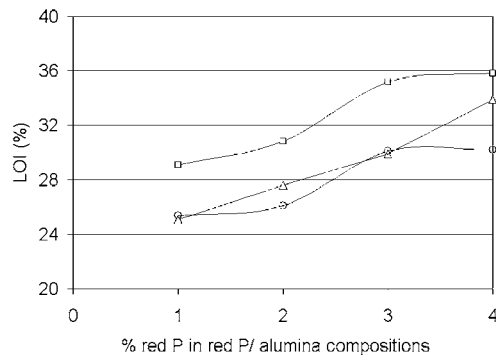


Fig. 7. Influence of the median diameter and specific surface area of alumina on the Limiting Oxygen Index of filled PET for several red P/alumina compositions. (△) red P, alumina (ATH calcinated at 700 °C) median diameter 2.5  $\mu\text{m}$ , sBET = 130  $\text{m}^2/\text{g}$ , synthetic alumina median diameter 0.5  $\mu\text{m}$ , sBET = 5.6  $\text{m}^2/\text{g}$ .

could take part in a chemical reaction involving phosphorus. We will now focus on the specific mechanism of action concerning  $\text{Al}_2\text{O}_3$ .

The above results with alumina were obtained using a calcined product. The conditions of calcination were 700 °C for 8 h. Due to this thermal treatment, the initial specific surface area of alumina hydroxide increased from 4 to 130  $\text{m}^2/\text{g}$ . A comparison was made between two aluminas with different specific surface areas and median particle sizes (respectively, 2.5  $\mu\text{m}$ , 130  $\text{m}^2/\text{g}$  for calcined Martinal and 0.5  $\mu\text{m}$ , 5.6  $\text{m}^2/\text{g}$  for Nabalco). The aluminas were incorporated in partial substitution of red P and the LOIs were measured.

Fig. 7 shows significant differences in LOI values between the two series of compositions differing only by the nature of  $\text{Al}_2\text{O}_3$  incorporated. In the case of the lower specific surface area, the synergistic effect disappears. One can also conclude that the influence of specific surface area is predominant over the particle size effect. This can be confirmed by using two types of alumina differing only in their specific surface area (respectively 130 and 250  $\text{m}^2/\text{g}$ ). These aluminas were obtained by changing the calcination conditions. The residue for 3% red P/2%  $\text{Al}_2\text{O}_3$  compositions studied by TGA (Fig. 8) is greater in the case of the higher specific surface area. This is favourable evidence for a catalytic effect of alumina.

The study of the IR spectra of chars obtained by combustion in a furnace at 500 °C with the same temperature profile as in TG experiments (Fig. 9) is likely to indicate if its chemical structure was modified by the presence of  $\text{Al}_2\text{O}_3$ . Chars corresponding to unfilled PET (a), PET containing 3% red P (b) and PET containing 3% red P + 2%  $\text{Al}_2\text{O}_3$  (c) were characterized. The specific features of the spectrum (a) can be more easily found on spectrum (c) than in spectrum (b). This can be interpreted by considering that the structure of char produced in the presence of alumina is relatively close to that formed in pure PET. Moreover, the P–O bonds are more present on spectrum (c) than in spectrum (b). This

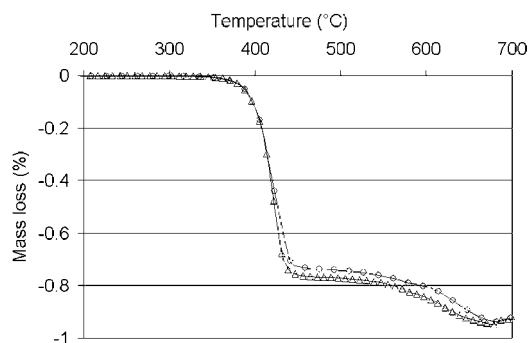


Fig. 8. TGA curves in air (5 °C/mn) of PET filled with 3% red P + 2% Alumina in function of the specific surface area of alumina, (○)  $\text{Al}_2\text{O}_3$  sBET = 250  $\text{m}^2/\text{g}$ , (△)  $\text{Al}_2\text{O}_3$  sBET = 130  $\text{m}^2/\text{g}$ .

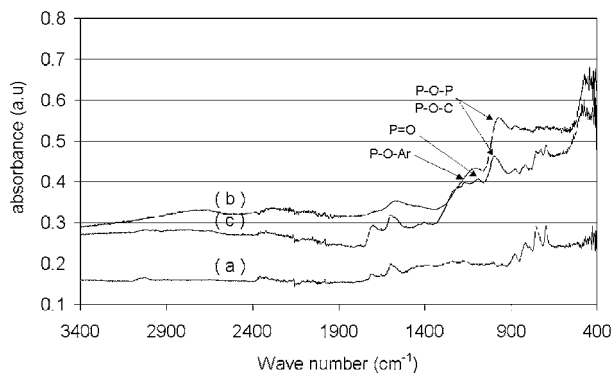


Fig. 9. (a) IRFT spectra of PET, (b) PET with 3% red P, (c) PET with 3% red P + 2% alumina.

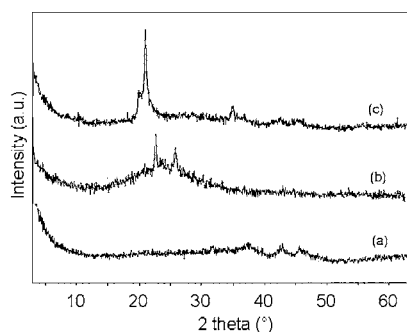


Fig. 10. X-ray spectra of (a) PET+Al<sub>2</sub>O<sub>3</sub>, (b) PET+red P, (c) PET+red P+Al<sub>2</sub>O<sub>3</sub>.

shows that the presence of alumina favours the oxidation of phosphorus, making it more active towards PET. In order to study the interactions between alumina and red P, the carbonaceous residues were studied by X-ray diffraction. However, in the spectrum corresponding to the residue after combustion at 500 °C and 5 °C/mn, the organic part of the residue prevents the analysis of a broad range of the X-ray spectrum. Consequently, the analysis was performed on a sample maintained for 3 h at 600 °C to eliminate this organic part corresponding to the PET residue. The X-ray spectra (Fig. 10) of compositions (b) and (c) exhibit some differences ascribed to the presence of:

- hydrogen phosphate (H<sub>4</sub>P<sub>2</sub>O<sub>7</sub>—ICDD n° 3-0275) in composition (b); and
- phosphorus oxide (P<sub>2</sub>O<sub>5</sub>—ICDD n° 23-1301) and aluminium phosphate (AlPO<sub>4</sub>—ICDD n° 11-0500) in composition (c).

Observations made using SEM and EDX on the residue of the (c) composition obtained at 500 °C also showed the presence of filamentous structures rich in phosphorus and oxygen, which could correspond to phosphorus oxide (Fig. 11). However, due to the small dimensions of these structures, it was not possible to determine their chemical nature by titration.

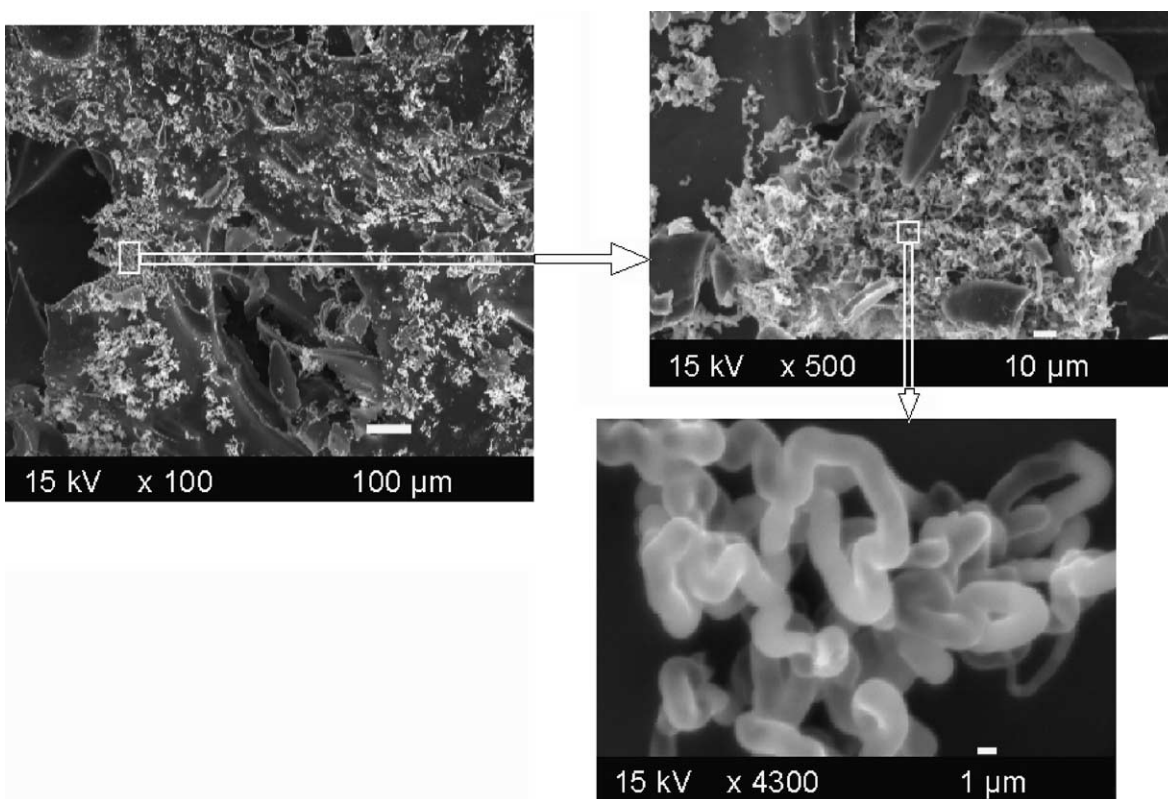


Fig. 11. SEM micrographs (×100, 500 and 4300) of the residue of (c) composition.

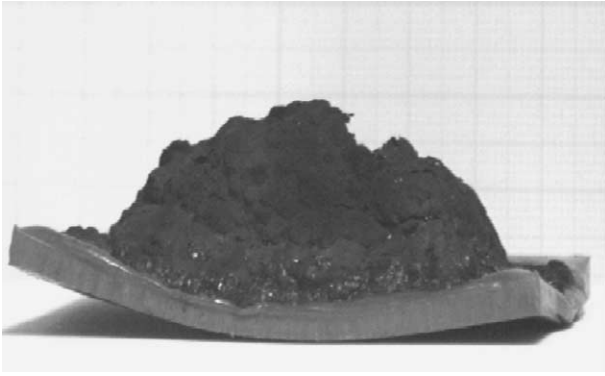


Fig. 12. Optical micrograph showing the intumescence for 3% red P + 6% glass fibres + 2%  $\text{Al}_2\text{O}_3$  in PET.

While the association of red P with metal oxides increases the LOI value of PET, no synergistic effect was observed using the epi-radiateur test. This result was ascribed to the low viscosity of the corresponding formulations, which leads to a flow of the molten polymer while it is charring. This phenomenon could also prevent a possible expansion of this char.

In a last series of experiments, we tried to obtain a mechanical stabilization of the char by incorporating a small quantity of reinforcing agent, glass fibres or talc. Talc has been used in some previous works to build mass diffusion barriers in FR systems [10].

The following additional compositions were produced:

- (d) 3% red P + 6% glass fibres in PET;
- (e) 3% red P + 6% glass fibres + 2%  $\text{Al}_2\text{O}_3$  in PET;
- (f) 3% red P + 6% talc in PET; and
- (g) 3% red P + 6% talc + 2%  $\text{Al}_2\text{O}_3$  in PET.

The observations of samples tested using the epi-radiateur show that the flow is significantly reduced and that intumescence occurs in the presence of both reinforcement agents, talc and glass fibres [Fig. 12, case of composition (e), similar to (g)]. No intumescence was observed for red P alone or in combination only with aluminium oxide due to the poor rheological properties of the char (flowing of the polymer surface).

Moreover, the presence of glass fibres or talc considerably lowered the RHR values (Fig. 5) and particularly the RHR peak for all the reinforced formulations. The best results were obtained for the ternary combination containing glass fibres. It was observed that glass fibres significantly increase the stiffness of the char layer formed and limit the flow of the molten material. Consequently, it can be considered that a good adhesion between the char layer and the glass fibres exists. In

addition, no chemical or morphological changes of glass fibres were observed when the intumescence process occurs. The positive role of reinforcements can be finally explained by the large amount of volatile combustibles which can be retained inside the char layer. This leads to the phenomenon of intumescence, which adds to the effect on fire resistance obtained by red P and  $\text{Al}_2\text{O}_3$ , which contributes to create the char.

#### 4. Conclusions

The upgrading of a recycled PET to obtain an engineered plastic requires removing impurities and drying the PET carefully to avoid a brittle material. The choice of encapsulated red phosphorus as flame retardant leads to interesting flammability results, nevertheless the use of increasing percentages of red phosphorus causes a strong decrease in impact resistance and an increase in the exothermicity for the first step of PET thermal degradation in air. The use of mineral oxides ( $\text{Al}_2\text{O}_3$ ,  $\text{MgO}$  and  $\text{Fe}_2\text{O}_3$ ) in substitution for red phosphorus can reduce the rate of heat release and improve LOI values. The action mechanism of these oxides is not based on an increase in viscosity. In the case of  $\text{Al}_2\text{O}_3$ , a physico-chemical action was highlighted, involving high specific surface areas and an influence on phosphorus oxidation. This effect was combined with an increase in viscosity using glass fibres and talc to favour the mechanical stability of the char and intumescence. A significant decrease in the rate of heat release was obtained in the case of ternary compositions and particularly in the presence of glass fibres.

#### References

- [1] Dinger P. Identiplast Conference, Brussels 23–24 April, 2001.
- [2] Muller AJ, Feijoo JL, Alvarez ME, Febles AC. *Polym Eng Sci* 1987;27:796.
- [3] Mullens J, Reggers G, Ruysen M, Carleer R, Yperman J, Van Poucke LC, Franco D. *J Thermal Anal* 1997;49:1061.
- [4] Gibert JP, Lopez Cuesta J-M, Bergeret A, Crespy A. *Polym Degrad Stab* 2000;67:437.
- [5] Zimmermann H. "Developments in polymer degradation". In: Grassie N. New York: Applied Science Publishers; 1984. p. 112.
- [6] Granzow A, Cannelongo JF. *J Appl Polym Sci* 1976;20:689.
- [7] Granzow A, Ferrillo RG, Wilson A. *J Appl Polym Sci* 1977; 21:1687.
- [8] Weil ED. 11th BCC Conference on Flame Retardancy, Stamford, CT, 22–24 May. 2000.
- [9] Yeh JT, Hsieh SH, Cheng YC, Yang MJ, Chen KN. *Polym Degrad Stab* 1998;61:399.
- [10] Durin-France A, Ferry L, Lopez Cuesta JM, Crespy A. *Polym Int* 2000;49:1101.